

Triphasic Ionic-Liquid Mixtures: Fluorinated and Non-fluorinated Aprotic Ionic-Liquid Mixtures

Oldamur Hollóczki,^[a] Marina Macchiagodena,^[a] Henry Weber,^[a] Martin Thomas,^[a] Martin Brehm,^[b] Annegret Stark,^[c] Olga Russina,^[d] Alessandro Triolo,^[e] and Barbara Kirchner^{*[a]}

We present here the possibility of forming triphasic mixtures from alkyl- and fluoroalkylimidazolium ionic liquids, thus, macroscopically homogeneous mixtures for which instead of the often observed two domains—polar and nonpolar—three stable microphases are present: polar, lipophilic, and fluorophilic ones. The fluorinated side chains of the cations indeed self-associate and form domains that are segregated from those of the polar and alkyl domains. To enable miscibility, despite the generally preferred macroscopic separation between fluorophilic

and alkyl moieties, the importance of strong hydrogen bonding is shown. As the long-range structure in the alkyl and fluoroalkyl domains is dependent on the composition of the liquid, we propose that the heterogeneous, triphasic structure can be easily tuned by the molar ratio of the components. We believe that further development may allow the design of switchable, smart liquids that change their properties in a predictable way according to their composition or even their environment.

1. Introduction

Ionic liquids (ILs)^[1] continue to be an exciting research topic because of their inherent wide chemical variety, which allows an unimaginable amount of new features to be discovered.^[2,3] One of the characteristic properties of ILs is their nanostructure, which was first observed from theoretical studies.^[4,5] In

subsequent experiments, microheterogeneity was proven by a low- q peak in the X-ray scattering of imidazolium-based ionic liquids.^[6]

Another exciting research field of ILs are their mixtures,^[7–12] which promise tuning of the properties by mixing different ILs with different desired properties. Macroscopically, several investigations have revealed nearly or even completely ideal mixing behavior for most of the systems.^[7–12] Although, on one hand, ideality makes the tuning of the properties of IL mixtures easier, novel properties are difficult to achieve, as the characteristics change between the extremes of the pure components. However, considering (especially local) microscopic structures,^[13,14] deviations from ideality can be detected. This has been confirmed by optical Kerr effect spectroscopy^[15] and theoretically by classical^[16] and ab initio^[13,14] molecular dynamics (MD) simulations. Furthermore, the non-ideal mixing behavior of hydrogen bonding in mixtures of protic ILs has been studied by far-IR spectroscopy measurements supported by MD simulations by the Ludwig group.^[10] In another article, a detailed MD analysis is given for the non-ideal mixing behavior explained by simple lattice models.^[17]

Thus, despite this often observed ideal macroscopic mixing behavior, several exciting applications are possible for which preferential solvation by, for example, hydrogen bonding gives rise to non-additive effects, which may lead to improvements in the performance of the given ILs relative to that of the pure components.^[7]

Beside mixing, the interesting features of ILs can also be altered by their functionalization.^[18,19] Many examples such as cation variation by ether,^[20,21] amide, nitrile,^[22] alcohol, or alkene functionalization of the side chain but also chirality^[23] have appeared in the literature. Amongst the several possibili-

[a] Dr. O. Hollóczki, Dr. M. Macchiagodena, H. Weber, M. Thomas, Prof. Dr. B. Kirchner
Mulliken Center for Theoretical Chemistry
Rheinische Friedrich-Wilhelms-Universität Bonn
Beringstr. 4+6, 53115 Bonn (Germany)
E-mail: kirchner@thch.uni-bonn.de

[b] Dr. M. Brehm
Helmholtz-Zentrum für Umweltforschung Leipzig
Department Ökologische Chemie
Permoserstrasse 15, 04318 Leipzig (Germany)

[c] Prof. Dr. A. Stark
SMRI Sugarcane Biorefinery Research Chair
University of KwaZulu-Natal College of Agriculture, Engineering and Science
School of Engineering
Howard College Campus, Durban (South Africa)

[d] Dr. O. Russina
Department of Chemistry, Sapienza University of Rome
00185 Rome (Italy)

[e] Dr. A. Triolo
Laboratorio Liquidi Ionici, Istituto Struttura della Materia
Consiglio Nazionale delle Ricerche
00133 Rome (Italy)

Supporting Information for this article is available on the WWW under <http://dx.doi.org/10.1002/cphc.201500473>.

© 2015 The Authors. Published by Wiley-VCH Verlag GmbH & Co. KGaA. This is an open access article under the terms of the Creative Commons Attribution Non-Commercial NoDerivs License, which permits use and distribution in any medium, provided the original work is properly cited, the use is non-commercial and no modifications or adaptations are made.

ties, fluorination has also been examined.^[24] Previously, we investigated fluorinated aprotic ionic liquids (FAILs),^[25,26] for which we showed that nanosegregation is enhanced upon fluorination,^[25] but beside the effect of the size or the remaining properties of the side chain, the nature of the anion also influences the microheterogeneous structure. Furthermore, we were able to show that our newly developed domain analysis tool implemented in our free software TRAVIS^[27] aids in understanding microheterogeneity in greater detail,^[26] that is, we were able to quantify the two nanophases (i.e. polar, nonpolar) and the triphilic systems (i.e. polar, alkyl, and fluorous) of fluorinated imidazolium-based ionic liquids.^[26]

Fluorination, in general, is especially interesting in the context of (macroscopically) biphasic systems containing a fluorous phase, introduced as a new concept in 1994 by Horváth and Rábai.^[28] The underlying principle of the fluorous biphasic systems is based on the tendency of fluorous media to form a separate phase, which can be highly advantageous in the separation of the components. Owing to structural changes, many examples are witnessed, in which fluorination—often based on the gauche effect^[29,30]—has a tremendous effect in organocatalysis.^[31,32] Furthermore, material design by fluorination is a hot topic in liquid-crystal research,^[33] for which it is applied in liquid crystal displays.^[34,35] Next to these interesting chemical applications, modification of the macroscopic properties is achieved by (per)fluorination, such as by increasing the density and viscosity in the case of hydrocarbons,^[25] whereas the vapor pressure increases and boiling points are lowered despite the higher molecular weight. (Per)fluorination results in low surface tension and a high capacity for dissolving gases. These new materials show low intensity interactions with non-fluorinated organic compounds, and they are inert both chemically and biologically. Owing to their very strong C–F bonds, an increase in rigidity and a decrease in polarity can be observed, which in turn provides high solubility and low-energy requirements for expelling the molecules and regenerating the solvent upon a decrease in pressure or/and an increase in temperature.^[36]

Having observed a separate macroscopic fluorous phase in molecular liquids,^[28] it is logical to assume that fluorinated ionic liquids form a fluorous microphase, similar to the above-discussed domains built of non-fluorinated alkyl chains, but these domains do not mix with that formed by the alkyl side chains.^[37,26] Indeed, a few articles suggesting the nanostructuring of the fluorous moieties were recently published.^[36–38] Rusina et al. showed that fluorous phases in FAILs exist from X-ray and NOE NMR spectroscopy data.^[37] For this purpose, especially cations with short side chains were chosen, combined with the (nonafluorobutanesulfonyl)imide or (trifluoromethanesulfonyl)imide anion.

Pereiro et al., on the other hand, used differential scanning calorimetry, rheology, and MD simulations to analyze two fluorinated ILs, namely, 1-hexyl-3-methylimidazolium perfluorobutanesulfonate and tetrabutylammonium perfluorobutanesulfonate.^[36] Recently, MD simulations of fluorinated protic ionic liquids^[38] indicated the existence of high structural heterogeneities.^[39]

Whereas the triphilic microheterogeneity that arises from the side chains of the anions and the cations already shows—as mentioned above—significant potential in nanotechnology, they are limited by the fact that the two phases can be built up only in a well-defined ratio, as the molar ratio of the two ions must always be 1:1 to maintain charge neutrality. Accordingly, the sizes of the domains—and therefore the degree of microheterogeneity and triphlicity—can only be tuned by altering the length of the side chains and the degree of fluorination, which are predetermined already at the synthesis of the IL. However, it might be desirable, for example, in a synthetic application to switch between the triphilic state and the normal dual-character (polar–nonpolar domains) state of ILs in a manner similar to that described by Horváth and Rábai,^[28] namely, the ability to switch between a one-phase mode and a fluorous biphasic system could be important for cases in which mass transfer between phases is rate limiting. Indeed, in such a case the structure, physicochemical, and solvation properties can be affected to a significant extent, which results in the ability to design smart liquids that can be switched easily if desired. Thus, it would be a significant leap forward in the application of such smart materials if the domains, thus, the degree of separation, or the sizes of the different phases could be altered or even switched by a much less involved way, for instance, by simply changing the temperature or by mixing fluorinated and non-fluorinated ILs. In the present paper, we investigate FAIL and IL mixtures of different mole fractions and at different temperatures (for the cation compounds, see Figure 1). We try to understand the degree of structuring from these approaches and whether it is possible to influence them.

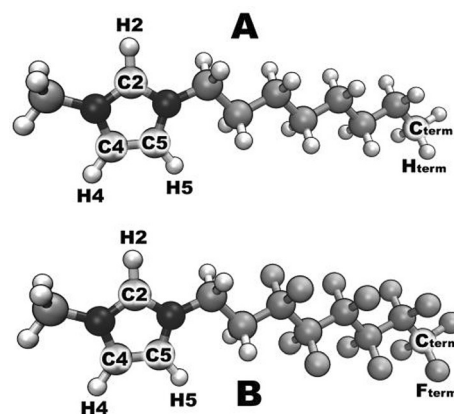


Figure 1. Atom labeling of the ions used in this work: a) $[\text{C}_8\text{C}_1\text{Im}]^+$ and b) $[(\text{C}_6)_2\text{C}_2\text{C}_1\text{Im}]^+$; bromide was chosen as the anion (not depicted).

Computational Methodologies and Implementation of Structure Factor

The details of the molecular dynamics simulations as well as some resulting quantities can be found in the Supporting Information.

Calculation of the theoretical structure factors $I(q)$ was implemented in TRAVIS^[27] according to Equation (1):

$$I(q) = \sum_{i=1}^N \sum_{j=1}^N x_i x_j f_i(q) f_j(q) H_{ij}(q) \quad (1)$$

with the partial structure factors [Eq. (2)]

$$H_{ij}(q) = 4\pi\rho_0 \int_0^{r_{\max}} r^2 (g_{ij}(r) - 1) \frac{\sin(qr)}{qr} dr \quad (2)$$

In these equations, r and q denote the distance and the wavevector modulus, respectively. The indices i and j run over the N different atom types in the simulation, x_i is the mole fraction of atom type i , $f_i(q)$ is the atomic scattering factor of atom type i , and $g_{ij}(r)$ is the radial distribution function of atom types i and j . The number density of atoms in the simulation is denoted by ρ_0 , and r_{\max} is the maximum sampled distance in the radial distribution function. The structure factors can be normalized to obtain Equation (3):

$$S(q) = \frac{I(q)}{\left(\sum_{i=1}^N x_i f_i(q)\right)^2} \quad (3)$$

or Equation (4):

$$S(q) = \frac{I(q)}{\sum_{i=1}^N x_i f_i(q)^2} \quad (4)$$

both normalizations are implemented in TRAVIS.^[27] Previously,^[40] it was shown that 300 ion pairs are enough to reproduce all features above 0.24 \AA^{-1} . However, as the scope of this work lies in the low- q region, we included two simulations at 423 and 300 K with 1024 ion pairs (see Table S1 in the Supporting Information), which still might be a critical number in terms of quantitative data.

2. Results

2.1. Mixing Alkyl- and Fluoroalkyl-Substituted ILs

Whereas the formation of triphasic structures has been previously observed and reported, any potential application of the so-far investigated ILs might be limited, as the extent of the segregation and the sizes of the different domains is predetermined at the stage of synthesis by the length of the alkyl (at the cation) and fluorinated (at the anion) side chains, as the ratio of the two functional groups is a constant 1:1. If, however, we could create such triphasic mixtures of the aforementioned FAILs and ILs, the microheterogeneous properties could also be altered and controlled by the molar ratio of the two liquids. This, however, requires that the two liquids are miscible to a reasonable extent, which is far from trivial.^[41] Whereas the idea of triphasicity is based on the general separation of hydrocarbons and fluorinated solvents, this very property can also limit the miscibility of FAILs and ILs,^[24] because differences in structures of either the anion or cation that are too large can give rise to two distinct macroscopic phases.^[41] Merrigan and Davis reported that the miscibility of partly fluorinated ionic liquids of the type $[(C_F)_n C_2 C_m \text{Im}][\text{PF}_6]$ with $n=6$ or 8 and $m=1$ or 4 in

Table 1. Miscibility of FAILs with ILs.

Entry	FAIL	IL	T [K]	Solubility [mol %]	Ref.
1	$[(C_F)_8 C_2 C_1 \text{Im}][\text{PF}_6]$	$[\text{C}_6 \text{C}_1 \text{Im}][\text{PF}_6]$	293	< 1	[24]
2	$[(C_F)_6 C_2 C_1 \text{Im}][\text{I}][\text{I}]$	$[\text{C}_6 \text{C}_1 \text{Im}][\text{I}][\text{I}]$	352	> 35	– ^[a]
3	$[(C_F)_8 C_2 C_1 \text{Im}][\text{PF}_6]$	$[\text{C}_{12} \text{C}_1 \text{Im}][\text{Tf}_2 \text{N}]$	293	> 10	– ^[a]
4	$[(C_F)_8 C_2 C_1 \text{Im}][\text{PF}_6]$	$[\text{C}_1 \text{C}_1 \text{Im}][\text{Tf}_2 \text{N}]$	293	> 10	– ^[a]

[a] Unpublished results.

the non-fluorinated 1-hexyl-3-methylimidazolium hexafluorophosphate $[(\text{C}_6 \text{C}_1 \text{Im}][\text{PF}_6])$ is surprisingly low (≈ 0.3 wt.%).^[24] Interestingly, in contrast to the previous findings, our qualitative results (Table 1) demonstrate that certain FAILs possess satisfying solubility in their non-fluorinated analogues.

Although from this preliminary data it is difficult to obtain any deep insight into the factors that control miscibility, it still suggests that—beside the clear effect of temperature,^[41] which affects largely the miscibility of fluorinated compounds with other substances^[28]—there must be a delicate interplay between hydrogen-bond donor/acceptor interactions, Coulombic interactions, and dispersion interactions. To understand the low solubility of the hexafluorophosphate-based ionic liquids (Table 1, entry 1), the way in which ILs mix should be kept in mind. Ideal mixing is observed for ions that feature similar properties in terms of size, steric demand, and ability to undergo interactions with other cations or anions.^[7] In fact, ideal mixing in the strict sense requires that the overall enthalpy of mixing is zero. Consequently, the sum of any newly formed interactions in the mixture, irrespective of their type (e.g. Coulombic, hydrogen bonding, dispersion), is equivalent to the magnitude of interactions present in both pure ionic liquids. $[\text{C}_6 \text{C}_1 \text{Im}][\text{PF}_6]$ is an isotropic liquid above its melting point,^[42] that is, a nonstructured liquid with relatively weak C2-H... $[\text{PF}_6]^-$ hydrogen bonding^[43,44] and normal alkyl-alkyl interactions owing to the chain length of six units.^[45,46] $[(C_F)_8 C_2 C_1 \text{Im}]^+$ has the same polar moieties, and therefore it similarly features few hydrogen-bonding interactions and a very high degree of fluoroalkyl chain dispersion interactions.

To obtain a macroscopically homogeneous solution, some interactions must exist to overcome the phobicity of the two different side chains. Thus, some linking cross interactions—implying interactions between the subunits of the two different liquids—must be possible either between the side chains or between the polar groups, which then allow interconnection of both liquids with a fluctuating network, that is, either dispersive forces or hydrogen bonding. However, as the fluorinated groups generally segregate or even separate from non-fluorinated moieties,^[28] solubility can only be achieved if the interactions between the polar groups enable the demixing effect of the mismatch between the side chains to be overcome. Accordingly, an extended hydrogen-bonding network must exist that would allow the cross interactions that are necessary for mixing. Given that the hydrogen-bonding ability depends strongly on the anion, by substituting the hexafluorophosphate with, for example, a halide (e.g. bromide, iodide)

anion—which are known to exhibit strong hydrogen-bonding interactions through the C2–H moiety^[44,47–53]—a mixed attractive interaction is introduced, and a counter balance to the phobicity between the fluoroalkyl and the alkyl side chain is given, which leads to (at least partial) miscibility. From this perspective, however, the solubility observed for the systems of entries 3 and 4 in Table 1 is intriguing, as the strength of the hydrogen bonds between the bis(trifluoromethylsulfonyl)imide anion ($[\text{Tf}_2\text{N}]^-$) and the acidic ring protons are under heavy debate.^[50,54] The $[\text{Tf}_2\text{N}]^-$ anion is observed to be almost as poor a hydrogen-bond acceptor anion as the $[\text{PF}_6]^-$ anion, and hence, the counter-balancing attractive interaction seems to be absent and little solubility should be achieved. On the other hand, the large, flexible, and fluorinated $[\text{Tf}_2\text{N}]^-$ anion might be capable of interacting with the fluoroalkyl chains (especially given that the fluorinated anion is introduced by the pure alkyl species, see Table 1), similar to the bis(pentafluoroethylsulfonyl)imide anion ($[\text{PF}_2\text{N}]^-$) presented in Ref. [26], which—as an alternative to the cross-IL hydrogen bonds—acts as a bridge between the two ionic liquids, leading to partial miscibility.

2.2. Densities

Comparing our simulated density (1.11 g cm^{-3}) of $[\text{C}_8\text{C}_1\text{Im}][\text{Br}]$ (see Table S1) to the one available at 300 K,^[55] we find better agreement (5% deviation) with the experiment (1.17 g cm^{-3}) than previous simulations.^[55] This might be due to the different charges or our smaller system size, which allow longer periods of equilibration. The simulated densities (see Table S1) increase with increasing fluorine content, as observed by both previous simulations^[56,25] and experiment.^[57]

For the characterization of the physical chemical properties of mixtures, discussing the density is generally a good starting point, because it contains valuable information about the packing effects and cross interactions within the system. Deviation from the ideal densities can be expressed by the excess molar volume (V^E). In non-fluorinated binary ionic liquid mixtures, positive V^E values are usually found,^[7] except for a few counter examples.^[58] The V^E values are generally small ($<0.1\%$), which indicates only slight structural rearrangements upon mixing,^[7] whereas somewhat larger values (0.1–0.5%) are obtained if the cations or anions are very unlike, for example, the alkyl chains are of very different lengths or the nature of the cations or anions are quite dissimilar. This has been assigned to nanosegregation by a combined molecular dynamics/attenuated total reflectance IR spectroscopy study.^[59,12]

In the present case, deviations in excess molar volume of up to -0.9% (Figure 2) are observed, which are notably higher than the values reported in experimental studies of other ionic-liquid mixtures. However, taking into account the extreme dissimilarity of the ions involved, this is not surprising. The obtained simulated densities are higher than ideal in most cases (V^E values are negative, see Figure 2). The negative V^E values indicate that the packing is more efficient and that the sum of favorable interactions is larger than that in the neat ILs.

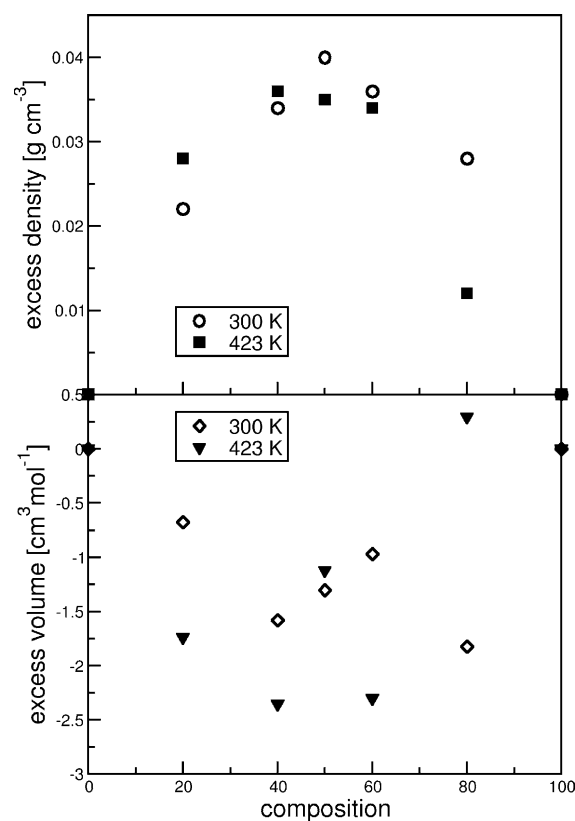


Figure 2. Top) Excess density and bottom) excess molar volume at different temperatures plotted with percentage of FAIL ($[(\text{C}_7)_6\text{C}_2\text{C}_1\text{Im}][\text{Br}]$) in IL ($[\text{C}_8\text{C}_1\text{Im}][\text{Br}]$).

This corresponds to favorable cross interactions that assist miscibility.

2.3. Structure Factor

Experimentally, the structure factor provides evidence for the long-range ordering of ILs with microheterogeneous structures; therefore, it is mandatory to predict it theoretically for our systems as well. The structure factor calculated for the 260 ion pair data at 300 and 423 K agrees well with the experimental data for pure $[\text{C}_8\text{C}_1\text{Im}][\text{Br}]$ ^[55] (see Figure 3, top), given that the cell consists of only 260 ion pairs. We observe peaks at $q = 5.4, 3.6, 1.5,$ and 0.27 \AA^{-1} , whereas the experimental values^[55] are located at $q = 5.8, 3.7, 1.6,$ and 0.29 \AA^{-1} for pure $[\text{C}_8\text{C}_1\text{Im}][\text{Br}]$; the peaks at $q = 0.27$ (calcd) and 0.29 \AA^{-1} (exptl) are characteristic of the aggregated side chains in microheterogeneous ILs. It was shown that by increasing the temperature a sizable shift to lower q values might be observed,^[40] which is also apparent upon comparing the gray solid (423 K) and black dashed (300 K) curves in Figure 3, top.

To discuss microheterogeneity itself, in Figure 3, bottom, the structure factor of the 50:50 mixture for the large system at 423 K is depicted. Most interestingly, we observe a double peak in the low q region at 0.45 and 0.25 \AA^{-1} (see left side of Figure 3, bottom), instead of the single peak at $q = 0.27 \text{ \AA}^{-1}$ observed in experiments on ILs with microheterogeneities.^[55] This

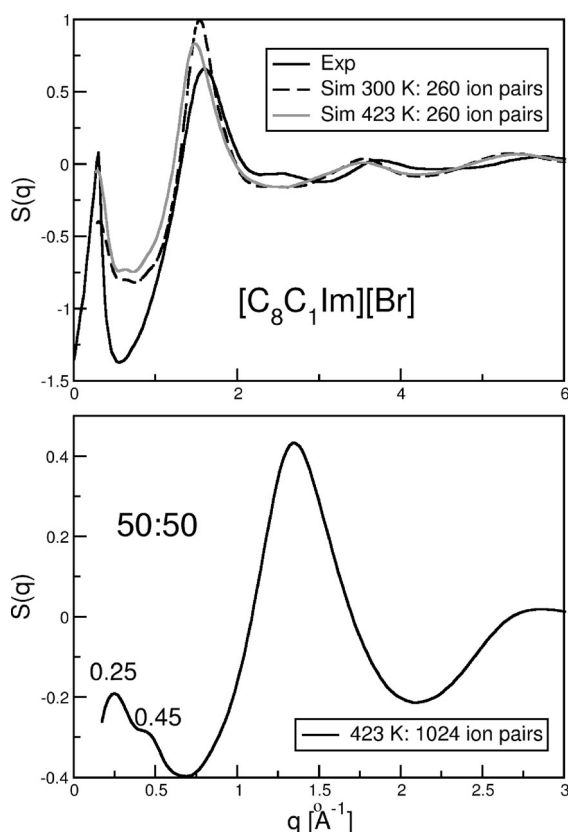


Figure 3. Top) Comparison of experimental (300 K) and calculated (300 and 423 K) structure factors from Equation (4) for pure $[\text{C}_8\text{C}_1\text{Im}][\text{Br}]$. Bottom) $S(q)$ as calculated from Equation (4) of 1024 ion pairs $[\text{C}_8\text{C}_1\text{Im}][\text{Br}]$ mixed with $[(\text{C}_7\text{F}_6\text{C}_2\text{C}_1\text{Im})][\text{Br}]$ in a 50:50 ratio at 423 K. The graph shows the low- q double-peak between 0.1 and 0.6 \AA^{-1} .

surprising result indicates that two different kinds of mesoscopic phases are present, and hence, these peaks are most likely to be associated with separate fluororous and alkyl phases. This double peak, as detected previously as well,^[36] might serve as another indication that the prepeak really fingerprints side-chain aggregation and is not only due to cation anisotropy (for a detailed discussion, see Ref. [40]).

In the bottom panel of Figure 3, the 1024 ion pair 50:50 simulation also exhibits a prominent peak at $q = 1.5 \text{ \AA}^{-1}$ (exptl: $q = 1.6 \text{ \AA}^{-1}$) next to the two smaller ones at $q = 0.25 \text{ \AA}^{-1}$ and 0.45 \AA^{-1} (the structure of the liquid with increasing FAIL content is given in the Supporting Information). Altogether it is difficult to establish any general trends in the changes in the peak positions with altering mole fraction.

2.4. Structure Depending on Mole Fraction

To investigate the structure in terms of the three phases (i.e. polar, fluororous, and alkyl), the radial distribution functions of $[\text{C}_8\text{C}_1\text{Im}][\text{Br}]$ and $[(\text{C}_7\text{F}_6\text{C}_2\text{C}_1\text{Im})][\text{Br}]$ together with their mixtures were analyzed. Given that these systems are characterized by long side chains, microheterogeneity is observable, and the bromide anion should also ensure a strong hydrogen-bonding network. The radial distribution functions (RDFs) corresponding to the $\text{C}2\text{--H}2\cdots\text{Br}$ hydrogen bonding at 423 K are shown in the Supporting Information. The details will not be discussed here, because hydrogen bonding in ionic liquids in general^[44,47–53] and upon fluorination^[25] has been analyzed elsewhere. Hydrogen bonding between the ring protons and the $[\text{Br}]^-$ anion is strongly observable in all systems. Independent of the fluororous content, hydrogen bonding appears to be similar, which suggests that the basic structure around the cationic head groups—so in the polar domains in general—is mostly unaffected by fluorination of the side chain and by the molar ratio of the two ILs. The location of the first, sharp peak is always at approximately $r = 290 \text{ pm}$, followed by a strong second peak at approximately $r = 630 \text{ pm}$, which corresponds to the other hydrogen bonds formed by the same cationic ring at the 4,5-positions. These hydrogen bonds also show prominent first peaks in the corresponding RDFs in the case of imidazolium-based ILs.^[44,47–51,53] Owing to the presence of these multiple hydrogen-bonding interactions, the existence of an extended hydrogen-bonding network can be surmised. The peak heights slightly, but monotonously, become larger as the molar ratio of the FAIL increases, which indicates that the higher fluorine content leads to stronger hydrogen bonds within both the FAILs and the ILs, although it has to be noted that the slower dynamics, namely, the higher viscosities, can also induce such effects, which was also reported for FAILs.^[25]

In Figure 4 representative snapshots of $[\text{C}_8\text{C}_1\text{Im}][\text{Br}]$ mixed with $[(\text{C}_7\text{F}_6\text{C}_2\text{C}_1\text{Im})][\text{Br}]$ are depicted for different compositions. It is clear that the fluorinated system shows more microheterogeneity than the parent ionic liquid (compare snapshots of

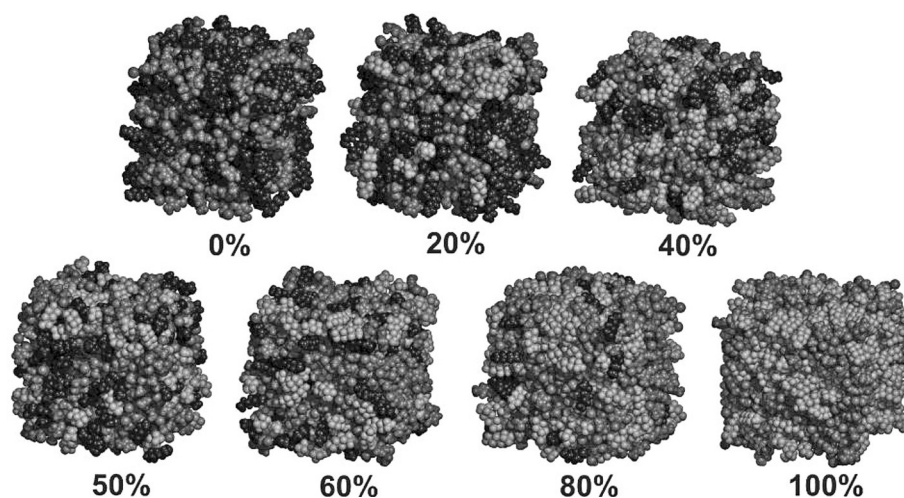


Figure 4. Grayscale snapshots of $[\text{C}_8\text{C}_1\text{Im}][\text{Br}]$ mixed with $[(\text{C}_7\text{F}_6\text{C}_2\text{C}_1\text{Im})][\text{Br}]$, simulated at 300 K. The percentage of the FAIL is indicated by the number below each system. For a colored snapshot see the Supporting Information.

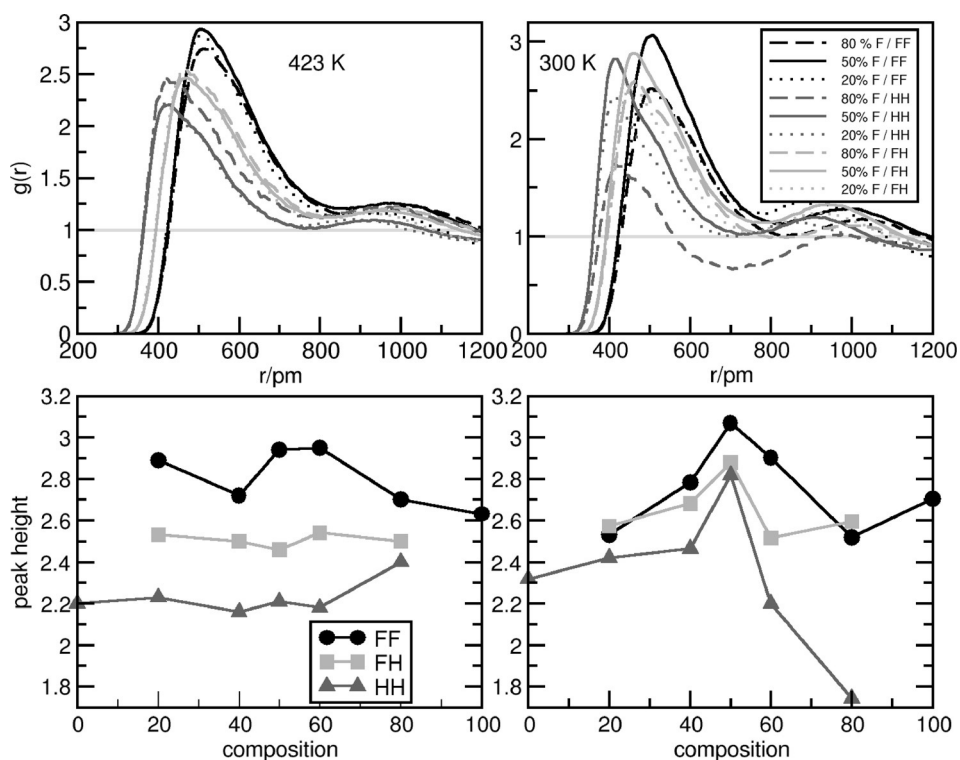


Figure 5. Selected radial distribution functions (left: 423 K, right: 300 K) of $[\text{C}_8\text{C}_1\text{Im}][\text{Br}]$ mixed with $[(\text{C}_F)_6\text{C}_2\text{C}_1\text{Im}][\text{Br}]$. FF indicates the $C_{\text{term}}-C_{\text{term}}$ function from the fluorinated side chains and HH indicates the $C_{\text{term}}-C_{\text{term}}$ function from the alkyl side chains, and FH indicates the $C_{\text{term}}-C_{\text{term}}$ function in which one carbon atom stems from the fluorinated side chain and the other one from the alkyl side chain. Bottom) Peak height plotted against the composition of the system. For color figures, see the Supporting Information.

compositions 0 and 100% in Figure 4). It is also apparent that the mixtures show microheterogeneity; however, the degree to which it occurs has to be determined from a more quantitative function. At first glance, it is also clear that the polar moieties and the side chains are segregated, and—in accordance with the previous results^[25]—this segregation is more dominant in the FAILs. Most remarkably, especially in the middle of the concentration range, the triphlicity is clearly visible, namely, in the 40–60% interval the alkyl, fluorous, and polar domains clearly form separate clusters in the simulation boxes.

After having seen the triphlicity in a qualitative way, the $C_{\text{term}}-C_{\text{term}}$ RDFs were calculated (see Figure 5: left for 423 K and right for 300 K). The most striking feature of these curves is that the first peaks do not change in height monotonously towards the larger FAIL contents. At both simulation temperatures, the strongest first neighbor interaction—at least for the fluorinated cation—is given approximately at the 50:50 mixture (Figure 5, bottom). From these data it is again apparent that the fluorinated side chains at any given composition always stick more together than the alkyl groups (compare FF and HH functions in Figure 5, F: fluorous; H: alkyl). The mixed interaction (FH curves, Figure 5) between the fluorous and alkyl side chain is always higher than the self-interaction of the alkyl side chain. At one composition (80:20) and temperature (300 K), the mixed interaction is even slightly more pronounced in the first peak height than the FF interaction.

The second shell peaks of the $C_{\text{term}}-C_{\text{term}}$ RDFs were also considered to characterize longer range nanostructuring. For the mixtures we find that at 423 K the fluorous side chain always provides the largest second shell peak, independent of the composition. In terms of composition, at the 50:50 and 20:80 mixtures the largest second neighbor peak is provided by the FF function followed by the mixed peak (FH) and by the HH peak. At the 80:20 fluorous content, the mixed peak is only as strong as the HH peak, and both are weaker than the FF peak. This is slightly different at 300 K. Although the FF second shell peak is always more intense than the HH peaks, the mixed interaction seems to be more pronounced than FF interaction at 50:50 and very weak at high fluorous content (80:20). The alkyl second peak is almost not present at low (20:80) fluorous content. All this information shows that the long-range structure is significantly influenced by the molar

ratio of the two components, which clearly suggests the possibility of tuning the structure and/or the behavior of the system by mixing.

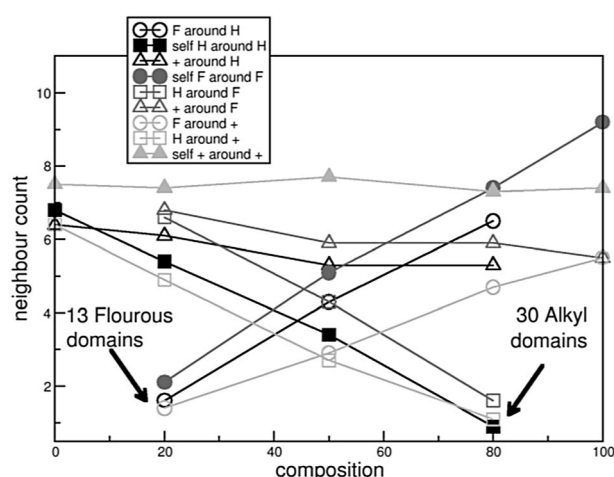


Figure 6. Neighbor count from Table 2 plotted against the composition of $[\text{C}_8\text{C}_1\text{Im}][\text{Br}]$ mixed with $[(\text{C}_F)_6\text{C}_2\text{C}_1\text{Im}][\text{Br}]$. F: “Fluorous”; H: “alkyl”, +: “ring” moieties. Black: neighbor count around “alkyl”, dark gray: neighbor count around “fluorous”, light gray: neighbor count around polar “ring” groups.

Table 2. Domain analysis at 300 K.^[a]

	System	Fluorous	Alkyl	Ring	Anion	Domain count	D-Vol [Å ³]	D-Surf [Å ²]	Q ^{peri}
fluorous	20:80	2.1	6.6	6.8	3.3	13.3	1090.9	902.9	0.51
	50:50	5.1	4.3	5.9	2.9	1.1	35 242.3	21 584.4	0.13
	80:20	7.4	1.6	5.9	2.8	1.0	58 423.8	26 288.7	0.15
	FAIL	9.2	–	5.5	2.7	1.0	74 523.9	24 086.9	0.21
alkyl	IL	–	6.8	6.4	3.2	1.0	47 800.1	26 340.6	0.12
	20:80	1.6	5.4	6.1	3.0	1.6	28 276.5	19 011.3	0.25
	50:50	4.3	3.4	5.3	2.5	6.2	43 671.1	36 166.6	0.47
	80:20	6.5	0.9	5.3	2.4	30.3	332.8	341.8	0.59
ring	IL	–	6.4	7.5	5.0	1.0	59 004.3	26 353.7	0.15
	20:80	1.4	4.9	7.4	5.0	1.0	59 024.8	25 943.6	0.15
	50:50	2.9	2.7	7.7	5.1	1.0	58 805.5	23 056.9	0.18
	80:20	4.7	1.1	7.3	5.0	1.0	58 971.1	24 617.2	0.16
	FAIL	5.5	–	7.4	5.0	1.0	59 014.7	24 086.9	0.17
anion	IL	–	3.2	5.0	0.2				
	20:80	0.7	2.4	5.0	0.2				
	50:50	1.4	1.2	5.1	0.2				
	80:20	2.3	0.5	5.0	0.3				
	FAIL	2.7	–	5.0	0.3				

[a] First column lists the group around which the neighbor count is performed. Next column gives the composition; columns three to six list the neighbor count. Next to the domain count, the domain volume (D-Vol) and domain surface (D-Surf) together with the average isoperimetric quotient (Q^{peri}) are given. Note for the last three columns the ring and anion are summarized as “polar group”; therefore, only data for the ring is given.

2.5. Domain Analysis

Finally, we present the data of the domain analysis to obtain a more quantitative picture of the triphasic microstructure of the mixtures (see Table 2 and Figure 6, the data for 423 K can be found in the Supporting Information). In the previous article, in which we developed the domain analysis,^[26] we showed that much more insight can be gained from this kind of data than from simply considering the RDFs. The subunits of the liquids are distinguished as discussed for the previous systems,^[26] namely, as “ring” and “anion” (which form together the polar domain), and as “alkyl” and “fluorous” (see also the Supporting Information).

With increasing FAIL content, the self-interaction between the “fluorous” subunits becomes higher, that is, in Table 2 a higher amount of neighbor count is found, which is depicted in Figure 6 (●). The “alkyl” unit behaves similarly in terms of self-contacts, as with decreasing concentration of the IL the “alkyl”–“alkyl” neighbors decrease in number (see Figure 6, ■). The neighbor counts are usually higher for the fluorinated side chains than for the alkyl groups (dark gray curves are usually higher than black curves in Figure 6), which is in good qualitative agreement with the peak heights in the RDFs for the interaction between the terminal carbon atoms. Interestingly, both side chains are surrounded by more polar groups (i.e. anion and cation) with decreasing fluororous content but the “fluorous” group is always enclosed by more polar groups than the “alkyl” side chain. However, in any composition, the polar group prefers self-aggregation over the surrounding of either the “alkyl” or the “fluorous” group (see the black, dark gray, light gray curves with triangles in Figure 6). The mixed interactions between the side chains behave like the self-interaction of the side chains, that is, with growing amount of FAIL/IL the amount of neighbors increases. The cationic head group

almost always possesses the higher self-neighbor count; thus, it is often surrounded by itself and by the anion, and the anion is also surrounded by the cation but not at all by other anions. The high neighbor count supports the idea of an extended network in the polar phase, which as a consequence might enable the macroscopic mixing of the IL with the FAIL.

Interestingly, as observed previously in other pure ionic liquids,^[60,26] the polar group always forms one domain in all mixtures and pure liquids, which deviates largely from sphericity, and again it shows an extended network of cationic head groups and anions. For the fluorinated side chains, there are fewer domains (at high FAIL content) than for the alkyl side chains (at high IL content), which again indicates that the fluororous side chains aggregate more intensely than the non-fluorinated ones. Most importantly, even at the higher temperature—apart from the 80:20 and 20:80 mixtures—the number of domains is generally low for all units, which suggests that triphasic liquids can be prepared by mixing ILs with fluorinated and non-fluorinated chains in the right ratio and at the right temperature.

It is important to note again that the first peaks between the fluorinated and the alkyl side chains are very high, in fact, higher than the first peaks in the alkyl–alkyl RDF. From this information it could be deduced that the nonpolar and fluororous side chains are miscible. In such a case, however, a large number of alkyl and fluororous domains are expected, which was not the case here (Table 2). Accordingly, the large mixed peaks should be interpreted rather through the neighboring alkyl and fluororous side chains at the surfaces of the two domains. This intriguing finding also clearly shows the necessity of our newly implemented domain analysis tool, which provides a much more sophisticated picture than considering only the corresponding RDFs.

If we concentrate on both points of dilute systems, that is, 20:80 and 80:20 FL/IL mixtures, we observe the following: at high IL content, “fluorous”–“fluorous” self-aggregation is low and “alkyl”–“alkyl” aggregation is high (as discussed above); the mixed interaction of “alkyl” around “fluorous” is even higher than the “alkyl”–“alkyl” self-interaction, whereas the mixed interaction of “fluorous” around “alkyl” is negligible. This behavior is almost the exact opposite to that found for the low IL content system, with the exception that the highest neighbor count is given for the “fluorous” self-interaction. Comparing these results together with the amount of domains to the behavior of the first peak in the RDF shows that the latter results have to be interpreted with care with respect to quantitative analysis.

3. Conclusions and Outlook

In this paper, we analyzed the structure of alkyl- and fluoroalkylimidazolium ionic liquid mixtures to build a basic theoretical framework for the design of ionic liquids with tunable or even switchable triphasic microheterogeneous structures; thus, with nanosegregation into three domains of polar, alkyl, and fluoroalkyl regions. As opposed to the previously designed triphasic ionic liquids (ILs) with the fluorinated tail attached to the anion and the non-fluorinated tail attached to the cation, we were motivated to create more room to tune this special nanoscale structure by allowing the ratio of the two kinds of side chains to change within a larger interval, which thus triggered triphasicity by forming mixtures. With this simple approach we can avoid predetermination of the characteristic sizes, structures, and association properties of the liquid at the synthesis stage by the length of the side chains, and these properties can be controlled upon application.

However, in a previous case^[26,37] of ILs with fluorinated anion–alkyl cation assemblies macroscopic homogeneity was achieved simply by naturally maintained charge neutrality, whereas in the case of the present mixtures, phase separation on the macroscopic scale can be induced by the very same fluorophobicity that may result in the interesting microscopic triphasic structure. We found, however, that strong interactions between the polar moieties of the two ionic liquids—in the case of strongly hydrogen-bonding anions—may counterbalance this separation behavior, which results in the desired macroscopically homogeneous but microscopically triphasic liquid. Indeed, in the case of the bromide anion the hydrogen-bonding behavior exhibited almost no selectivity for either of the two cations, and it instead provided an extended network, whereas the association of the side chains suffered significant structural changes.

The newly implemented domain analysis^[26] in TRAVIS^[27] allowed the analysis of the domains in terms of their numbers and their shapes. The polar region (including the anion and the head group of the cation) form a single domain in the pure liquids and all mixtures in the form of lengthy, nonspherical channels. The side chains, however, show completely different aggregation behavior. As the amount of the fluorinated ionic liquid is increased in the obtained macroscopically homo-

geneous mixtures, the heterogeneous microstructure of the pure non-fluorinated liquid is maintained, whereas the fluorinated side chains also start to associate to form a third, fluorinated microphase in the liquid. In the middle of the concentration range, therefore, these three phases coexist, but with a further increase in the molar ratio of the fluorinated IL the non-fluorinated IL becomes more dispersed and forms many independent clusters in the solution. In good agreement with these data and in clear contrast to the measurements that were conducted on pure ILs, the simulated structure factors exhibit a double low q peak, which shows the coexistence of two different kinds of long-range order corresponding to the aggregated fluorinated and alkyl domains.

Similar to that previously observed for IL mixtures that possess different side chains, and thus, different aggregation behavior, some deviations from ideality can be expected. Indeed, as the association behavior of the different side chains alters with the molar fractions, the densities show non-ideal behavior that is larger than that for other ionic-liquid mixtures.

As presented in our data, it seems possible to switch this triphasic association on the nanoscale in mixtures of fluorinated and non-fluorinated ionic liquids simply by varying the concentrations. Our study has several implications. Such a switchable triphasic mixture might be utilized in many ways. In the case of reactions that can be performed in only one of the three microphases, building or dispersing (i.e. destroying) these domains might have significant value. By adding one of the IL components to the reaction mixture one of the microphases can be dispersed, and the product will have to choose another phase, and thus, a transfer of compounds from one phase to the other takes place. By such directed transfer of the substances from one microphase to the other, one can switch the given chemical process on and off, or alternatively, reactions might be conducted in a selective and consecutive way by allowing collision with only certain kinds of molecules at a time. Similarly, by switching the triphasicity or the microheterogeneity in general, the solubility of a given substance in the IL phase could be altered, which would allow separation processes or selective synthesis. This concept might even work in mixtures of ILs with alkyl and polar side chains, as mentioned in the Introduction. By adding an IL with polar side chains, the microheterogeneity can be disintegrated and captured substances can be released. The same might be valid for mixtures of ILs with molecular liquids, which increase or decrease the microheterogeneity properties.

We believe that this rather simple principle will contribute to the overlapping fields of IL research, fluorine chemistry, and smart materials; furthermore, control over nanostructure can be gained, which might be considerably useful for the corresponding applications.

Acknowledgements

B.K. would like to thank the Deutsche Forschungsgemeinschaft (DFG) for support under the SPP 1708 project KI768/12-1, and support of the DFG through project KI 768/8-1 is also gratefully

acknowledged. B.K. and H.W. gratefully acknowledge the Fonds der chemischen Industrie. A.T. and O.R. acknowledge support from Fondo per gli investimenti della ricerca di base (FIRB) (RBF086BOQ) and Progetti di Ricerca di Interesse Nazionale (PRIN) (2009WHPHRH). A.S. would like to thank the Deutsche Forschungsgemeinschaft for support (STA 1027/6-1) We would all like to acknowledge the kind support in the framework of the COST Action EXIL—Exchange on Ionic Liquids (CM1206). We thank Prof. J. H. Davis (Univ. of South Alabama) for kindly providing a generous sample of the fluorinated sample $[(C_7)_8C_2C_1Im][PF_6]$.

Keywords: ionic liquids · microphases · molecular dynamics · nanosegregation fluorination · simulations microheterogen

- [1] T. Welton, *Chem. Rev.* **1999**, *99*, 2071–2083.
 [2] E. Vanecht, K. Binnemans, J. W. Seo, L. Stappers, J. Fransaer, *Phys. Chem. Chem. Phys.* **2011**, *13*, 13565–13571.
 [3] K. Binnemans, *Chem. Rev.* **2007**, *107*, 2592–2614.
 [4] Y. Wang, G. Voth, *J. Am. Chem. Soc.* **2005**, *127*, 12192–12193.
 [5] J. N. C. Lopes, A. A. H. Pádua, *J. Phys. Chem. B* **2006**, *110*, 3330–3335.
 [6] A. Triolo, O. Russina, H.-J. Bleif, E. D. Cola, *J. Phys. Chem. B* **2007**, *111*, 4641–4644.
 [7] A. Stark, M. Brehm, M. Brüssel, S. Lehmann, A. Pensado, M. Schöppke, B. Kirchner, *Top. Curr. Chem.* **2013**, *351*, 1–39.
 [8] H. Niedermeyer, J. P. Hallett, I. J. Villar-Garcia, P. A. Hunt, T. Welton, *Chem. Soc. Rev.* **2012**, *41*, 7780–7802.
 [9] G. Chatel, J. F. B. Pereira, V. Debbeti, H. Wang, R. D. Rogers, *Green Chem.* **2014**, *16*, 2051–2083.
 [10] K. Fumino, A.-M. Bonga, B. Golub, D. Paschek, R. Ludwig, *ChemPhysChem* **2015**, *16*, 299–304.
 [11] M. Y. Lui, L. Crowhurst, J. P. Hallett, P. A. Hunt, H. Niedermeyer, T. Welton, *Chem. Sci.* **2011**, *2*, 1491–1496.
 [12] M. T. Clough, C. R. Crick, J. Grasvik, P. A. Hunt, H. Niedermeyer, T. Welton, O. P. Whitaker, *Chem. Sci.* **2015**, *6*, 1101–1114.
 [13] M. Brüssel, M. Brehm, T. Voigt, B. Kirchner, *Phys. Chem. Chem. Phys.* **2011**, *13*, 13617–13620.
 [14] M. Brüssel, M. Brehm, A. S. Pensado, F. Malberg, M. Ramzan, A. Stark, B. Kirchner, *Phys. Chem. Chem. Phys.* **2012**, *14*, 13204–13215.
 [15] D. Xiao, J. R. Rajian, L. G. Hines, S. Li, R. A. Bartsch, E. L. Quitevis, *J. Phys. Chem. B* **2008**, *112*, 13316–13325.
 [16] K. Shimizu, M. Tariq, L. P. N. Rebelo, J. N. C. Lopes, *J. Mol. Liq.* **2010**, *153*, 52–56.
 [17] D. Paschek, B. Golub, R. Ludwig, *ChemPhysChem* **2015**, *17*, 8431–8440.
 [18] J. Davis, Jr., *Chem. Lett.* **2004**, *33*, 1072–1077.
 [19] J. Davis, K. Forrester, *Tetrahedron Lett.* **1999**, *40*, 1621–1622.
 [20] A. Triolo, O. Russina, R. Caminiti, H. Shirota, H. Y. Lee, C. S. Santos, N. S. Murthy, E. W. Castner, Jr., *Chem. Commun.* **2012**, *48*, 4959–4961.
 [21] K. Shimizu, C. E. S. Bernardes, A. Triolo, J. N. C. Lopes, *Phys. Chem. Chem. Phys.* **2013**, *15*, 16256–16262.
 [22] K. C. Lethesh, K. Van Hecke, L. Van Meervelt, P. Nockemann, B. Kirchner, S. Zahn, T. N. Parac-Vogt, W. Dehaen, K. Binnemans, *J. Phys. Chem. B* **2011**, *115*, 8424–8438.
 [23] M. B. Foreiter, H. Q. N. Gunaratne, P. Nockemann, K. R. Seddon, G. Srinivasan, *Phys. Chem. Chem. Phys.* **2014**, *16*, 1208–1226.
 [24] T. Merrigan, E. Bates, S. Dorman, J. Davis, *Chem. Commun.* **2000**, 2051–2052.
 [25] H. Weber, O. Hollóczki, A. S. Pensado, B. Kirchner, *J. Chem. Phys.* **2013**, *139*, 084502.
 [26] M. Brehm, H. Weber, M. Thomas, O. Hollóczki, B. Kirchner, *ChemPhysChem* **2015**, DOI: 10.1002/cphc.201500471.
 [27] M. Brehm, B. Kirchner, *J. Chem. Inf. Model.* **2011**, *51*, 2007–2023.
 [28] I. Horváth, J. Rábai, *Science* **1994**, *266*, 72–75.
 [29] M. Tavasli, D. O'Hagan, C. Pearson, M. C. Petty, *Chem. Commun.* **2002**, 1226–1227.
 [30] S. Paul, W. B. Schweizer, G. Rugg, H. M. Senn, R. Gilmour, *Tetrahedron* **2013**, *69*, 5647–5659.
 [31] L. E. Zimmer, C. Sparr, R. Gilmour, *Angew. Chem. Int. Ed.* **2011**, *50*, 11860–11871; *Angew. Chem.* **2011**, *123*, 12062–12074.
 [32] A. Berkessel, J. A. Adrio, *J. Am. Chem. Soc.* **2006**, *128*, 13412–13420.
 [33] K. Binnemans, *Chem. Rev.* **2005**, *105*, 4148–4204.
 [34] P. Kirsch, M. Bremer, *ChemPhysChem* **2010**, *11*, 357–360.
 [35] M. Bremer, P. Kirsch, M. Klasen-Memmer, K. Tarumi, *Angew. Chem. Int. Ed.* **2013**, *52*, 8880–8896; *Angew. Chem.* **2013**, *125*, 9048–9065.
 [36] A. B. Pereira, M. J. Pastoriza-Gallego, K. Shimizu, I. M. Marrucho, J. N. C. Lopes, M. M. Pineiro, L. P. N. Rebelo, *J. Phys. Chem. B* **2013**, *117*, 10826–10833.
 [37] O. Russina, F. L. Celso, M. D. Michiel, S. Passerini, G. B. Appetecchi, F. Castiglione, A. Mele, R. Caminiti, A. Triolo, *Faraday Discuss.* **2013**, *167*, 499–513.
 [38] Y. Shen, D. F. Kennedy, T. L. Greaves, A. Weerawardena, R. J. Mulder, N. Kirby, G. Song, C. J. Drummond, *Phys. Chem. Chem. Phys.* **2012**, *14*, 7981–7992.
 [39] J. J. Hettige, H. K. Kashyap, H. V. R. Annapureddy, C. J. Margulis, *J. Phys. Chem. Lett.* **2013**, *4*, 105–110.
 [40] H. V. R. Annapureddy, H. K. Kashyap, P. M. De Biase, C. J. Margulis, *J. Phys. Chem. B* **2010**, *114*, 16838–16846.
 [41] A. Arce, M. J. Earle, S. P. Katdare, H. Rodriguez, K. R. Seddon, *Chem. Commun.* **2006**, 2548–2550.
 [42] C. M. Gordon, J. D. Holbrey, A. R. Kennedy, K. R. Seddon, *J. Mater. Chem.* **1998**, *8*, 2627–2636.
 [43] W. Zhao, F. Leroy, B. Heggen, S. Zahn, B. Kirchner, S. Balasubramanian, F. Müller-Plathe, *J. Am. Chem. Soc.* **2009**, *131*, 15825–15833, PMID: 19827790.
 [44] A. Stark, M. Sellin, B. Ondruschka, K. Massonne, *Sci. China Chem.* **2012**, *55*, 1663–1670.
 [45] M. Macchiagodena, L. Gontrani, F. Ramondo, A. Triolo, R. Caminiti, *J. Chem. Phys.* **2011**, *134*, 114521.
 [46] B. Kirchner, O. Hollóczki, J. C. Lopes, A. Pádua, *WIREs Comp. Mol. Sci.* **2014**, 202–214.
 [47] P. A. Hunt, B. Kirchner, T. Welton, *Chem. Eur. J.* **2006**, *12*, 6762–6775.
 [48] P. A. Hunt, *J. Phys. Chem. B* **2007**, *111*, 4844–4853.
 [49] S. B. C. Lehmann, M. Roatsch, M. Schoppke, B. Kirchner, *Phys. Chem. Chem. Phys.* **2010**, *12*, 7473–7486.
 [50] V. Kempter, B. Kirchner, *J. Mol. Struct.* **2010**, *972*, 22–34.
 [51] A. Stark, *Top. Curr. Chem.* **2010**, *290*, 41–81.
 [52] O. Hollóczki, D. Gerhard, K. Massone, L. Szarvas, B. Németh, T. Veszprémi, L. Nyulászi, *New J. Chem.* **2010**, *34*, 3004–3009.
 [53] O. Hollóczki, L. Nyulászi, *Org. Biomol. Chem.* **2011**, *9*, 2634–2640.
 [54] R. Cooper, A. M. Zolot, J. A. Boatz, D. P. Sporleder, J. A. Stearns, *J. Phys. Chem. A* **2013**, *117*, 12419–12428.
 [55] E. Bodo, L. Gontrani, A. Triolo, R. Caminiti, *J. Phys. Chem. Lett.* **2010**, *1*, 1095–1100.
 [56] G. D. Smith, O. Borodin, J. J. Magda, R. H. Boyd, Y. Wang, J. E. Bara, S. Miller, D. L. Gin, R. D. Noble, *Phys. Chem. Chem. Phys.* **2010**, *12*, 7064–7076.
 [57] R. Singh, S. Manandhar, J. Shreeve, *Synthesis* **2003**, 1579–1585.
 [58] P. Navia, J. Troncoso, L. Romaní, *J. Chem. Eng. Data* **2007**, *52*, 1369–1374.
 [59] S. Aparicio, M. Atilhan, F. Karadas, *Ind. Eng. Chem. Res.* **2010**, *49*, 9580–9595.
 [60] K. Shimizu, C. E. S. Bernardes, J. N. C. Lopes, *J. Phys. Chem. B* **2014**, *118*, 567–576.

Manuscript received: March 6, 2015

Revised: July 16, 2015

Final Article published: August 25, 2015